10.2478/tvsb-2014-0014

Transactions of the VŠB – Technical University of Ostrava

No. 2, 2014, Vol. 14, Civil Engineering Series

paper #14

Dimitra ACHILLOPOULOU[1], Theodoros PARDALAKIS[2], Athanasios KARABINIS[3]

INTERFACE CAPACITY OF REPAIRED CONCRETE COLUMNS STRENGTHENED WITH RC JACKETS

Abstract

The study describes the retrofit of repaired elements by reinforced concrete (RC) jacketing conducted to quantify the influence of initial construction deficiencies and of different type of anchors to the ability of the interface to transfer loads. Sixteen specimens (section scale 1:2) were designed with variables the initial deficiencies and the confinement ratio. The results indicate that: a) the maximum resistance load and dissipated energy of initially damaged specimens are decreased; b) surpassing a specific amount of damage, columns even suitably repaired present lower strain capacity, c) welded bars lead to buckling of longitudinal bars.

Keywords

Concrete jacket, construction damage, repair and strengthening, dowels, welded bend down bars.

1 INTRODUCTION

Numerous techniques have been applied in upgrading and rehabilitating the capacity of crucial of the reinforced concrete (RC) elements, such as columns. Jacketing with various materials such as FRPs and reinforced concrete jackets (high strength concrete, self-consolidating, etc.) is commonly used in seismic retrofitting [1], [2], [3], [4]). The key of the strengthening design has proven to be the interface capacity in transferring loads and to slip [5], [6], [7], [8]). For this reason it is commonly adopted the treatment of the interface with various methods [9]. Either by increasing the roughness [10] of the surface or by applying bonding resins [11] or even finally by placing steel connectors of various kinds [12], [13], [14] the interface capacity is considered to be enhanced [15], [16].

Various codes world-widely [17], [18]: *Greek Retrofit Code Attuned to EN 1998/3*, [19] do not quantify the resistance load of elements repaired with each rehabilitation method. Moreover, in all published studies the variable overloading effect [20] is usually examined, though, the factor of extensive construction damage in combination with loading influence is not very analytically referred to [21], [22]. It is decided to quantify and examine the influence of the latter factor to the interface surface in bearing and transferring loads. Together with the initial damage factor, the kind of connectors placed at the interface is studied. Dowels and bend down welded bars were selected to connect the interface of the jacketed elements.

The current study adds useful information to previous studies [20], [21] and clarifies the influence of damages to the bearing capacity after repair and therefor retrofitting, the failure mechanisms are defined after repair and strengthening.

[1] Dimitra Achillopoulou Dr, MSc Civil Engineer, Civil Engineering Department, Democritus University of Thrace, Vas. Sofias 12, 67100, Xanthi, Greece, phone: +30 25410 79688, e-mail: dimiachi@civil.duth.gr.

[2] Theodoros Pardalakis, MEng, Civil Engineering Department, Democritus University of Thrace, Vas. Sofias 12, 67100, Xanthi, Greece, e-mail: theopardalakis@gmail.gr.

[3] Athanasios Karabinis, Professor, Civil Engineering Department, Democritus University of Thrace, Vas. Sofias 12, 67100, Xanthi, Greece, phone: +30 25410 79666, e-mail: karabin@civil.duth.gr.

2 EXPERIMENTAL PROGRAM

The research presented in this paper examines and quantifies the influence of damages to the behavior of the repaired column and to the retrofitted one when upgrading is decided. What is more, in order to ensure monolithic behavior between old and new concrete connectors are usually placed. The failure mechanisms of each kind of connector are investigated together with their capacity in transferring loads. The real condition of loading was simulated. The old column is directly loaded and transfers loads to the jacket. Even when the jacket has the same height with the original column, the shrinkage effect of the different time casted concretes will again lead to the aforementioned situation. Shrinkage though is not quantified but the phenomenon is taken into consideration at the loading approach. The shrinkage of old concrete is assumed to have grown in the hardening period. As far as jacket concrete is concerned, the phenomenon is assumed to be eliminated by the old concrete lateral expansion. In both cases, values are negligible. A comparison with the assumed monolithic loading pattern was made.

2.1 Investigation of initial construction damage

Sixteen specimens were built to simulate reinforced concrete columns (cores) in section scale 1:2 of rectangular section 150x150 mm and height 500 mm. The variables studied were:

1) Initial construction damage

2) Stirrups spacing

3) Kind of interface reinforcement

4) Load Pattern influence

The material used were concrete of approximately 24 MPa nominal strength measured cylinder specimens at 28 days, 566 MPa yield stress for longitudinal reinforcement and 250.76 MPa for stirrups. Specimens were symmetrically reinforced with two bars of 8 mm diameter at each face (Fig. 1). Transverse reinforcement consisted of 5.5 mm diameter spaced at 100 mm or 50 mm. All steel bars were adequately anchored.

During casting consolidation of concrete was incomplete in order to create initial construction damages in 9 columns (Fig. 2). Casting was not performed according to the provisions set by EN 206-1 [22] and ACI 309R-06 [23] as in real construction sites where it is common to ignore the standards set. According to international standards of concrete consolidation through internal vibration for application of plastic concrete in thin members and confined areas the use of a 20-40 mm head diameter vibrator is suggested. In this way, the radius of action is 80-150 mm. What is more, the rate of concrete placement is assumed to be within 920-4600 mm in the current study, a 20 mm head diameter vibrator was used and concrete was being placed in higher frequency than predicted. Five specimens were constructed healthy and considered as reference models. Damaged specimens were repaired using high strength thixotropic concrete and were subjected to axial compression repeatedly with cycles of 1‰ axial strain up to 10‰. This pre-loading procedure created cracks as found in real structure members before retrofitting. The axial deformation was measured from the relative displacements between two loading platens with the use of Displacement Transducers (D.T.). The axial load is applied in a compression machine with a capacity of 3000 kN maximum load (Fig. 3).

2.2 Investigation of strengthening through RC jacketing

Jackets were added to three repaired specimens and to four healthy identical ones. Specimens are categorized in three sets according to:

1) Load Pattern

2) Kind of connectors of the interface

3) Stirrups ratio

Jackets of 80 mm (3.15 in) were placed at all four faces made of 31MPa nominal stress. Again the cross section was symmetrically reinforced with two 8 mm longitudinal bars and stirrups

spaced at 100 mm and 25 mm (Fig. 4). All steel bars were of the same quality class with the steel of the cores. The size of jacket was decided in order to create enough anchorage length for the steel connectors placed.

Steel connectors of different kind were selected in order to investigate their efficiency in transferring loads. Eight specimens were selected for retrofitting. In two repaired and retrofitted ones six dowels of 10 mm (0.394 in) were placed, symmetrically at the two opposite faces (Fig. 4a). Three healthy identical ones also contained dowels. In three healthy specimens, before the jacket was casted the longitudinal bars were welded together with bend down bars of 8 mm diameter (Fig. 4b). Steel connectors were designed according to the minimum percentages indicated by EN-1998/3 [17], [18] ($\rho_{\delta min} \geq 1.2$ ‰). ACI-318R-08 [19] provides only the shear resistance of the interface but not the minimum percentage of steel crossing it [$V_n = A_{vf} f_y (\mu \sin \alpha + \cos\alpha)$]. An epoxy resin (EN 1504 [24] [(Bond strength 14 days: 15.1 MPa (2200 psi), compressive strength 28 days, 23°C: 84.1 MPa, Shear strength ASTM D732 24.8 MPa] was applied as a bonding agent at the interface of old and new concrete since no other preparation was adopted. In fact, in previous study [21], epoxy resin was proven to act effectively and favourably to the transferring load capacity (Table 1– Specimens' characteristics Table 1).

Two different Load Patterns were selected (Fig. 7):

• Load Pattern B (B): Direct loading of core with the entire retrofitted element supported. That case simulates the function of a retrofitted column of a real structure where the growth of the axial load happens through the old column (core).

• Load Pattern D (D): Direct loading of both core and jacket in order to investigate the mechanical behavior of the jacketed column considered as monolithic.

Even though jacketed elements bear seismic loads, for the investigation of the interface all specimens were subjected to axial compression.

3 INITIAL CONSTRUCTION DAMAGE EFFECT

The results of tests conducted take into consideration the stress-strain curves, or P-δ curves and failure mechanisms obtained directly by measurements and observation and finally the capacity in dissipating energy up to peak load and on the whole obtained indirectly by calculations. In Fig. 8 the role of stirrups is depicted specimen designed without high ductility requirements (R_c-2, ω_{wc}=0.075) representing older codes' approaches of confinement is compared with an identical one (R_c-1) designed closer to modern codes (ductility orientated codes: higher percentages of stirrups- ω_{wc}=0.15). In both classifications the yielding strain is 2.7 ‰. At these strain levels, the mechanism of confinement is fully activated and its role is dominant for the crushing level of concrete. These specimens with higher ratio of stirrups according to new codes lead to 13 % higher axial stress for strains up to 10 ‰. Both specimens achieved the maximum resistance stress (peak stress) at 7 ‰ strain. Specimen with low percentages of stirrups (R_c-2) presents an abrupt descending branch. In contrast to, the presence of denser stirrups (R_c-1) lead to a plastic branch with low reduction of maximum resistance (8 %). Specifically, the nominal displacement ductility factor μ_δ, ($\mu_\delta = \frac{\delta u}{\delta peak}$) achieved equals 3.68 meaning 25% higher than specimen R_c-2.

3.1 Proposed quantification of construction damages

In order to quantify the construction damages a simple model was developed by authors. The penetration of damage in the section and its expansion along the height of specimens was measured (Fig. 9). The percentages of those damages to the designed dimensions are extracted through three different indexes:

I) Section index d_s is the damage ratio of the section (Eq. 1)

II) Axial index d_h which quantifies the expansion axially (Eq.2) and,

III) Volumetric index d_v (Eq.3) which combines the above-mentioned indexes resulting to the volumetric ratio of damage.

$$d_s = \frac{f_1}{f_{tot}} \quad (1)$$

$$d_h = \frac{h_1}{h_{tot}} \quad (2)$$

$$d_v = 1 - [(1 - d_s) \times (1 - d_h)] \quad (3)$$

Table 2–Specimens' characteristics shows analytically the damage indexes for specimens with low ductility requirements (low ratio of stirrups) and for specimens with ductility requirements (higher ratio of confinement).

3.2 Performance of damaged specimens

The effect of construction damages in repeated loading of low ductility specimens is shown in Fig. 10. Again, up to 3‰ axial strain all coincide. At strain greater than 3 ‰ specimens highly damaged (d_s index, Table 1: D_mR_c-1, D_mR_c-2, D_mR_c-3) present lower values of maximum stress than the healthy one (R_c-2). All stress-strain curves have peak stress at 7 ‰ strain. After peak, the damaged specimens present a steady plastic branch. The healthy specimen after 8 ‰ strain loses its capacity and the curve declines abruptly. It is noticed that for the same levels of repaired section (d_s=25 %) specimens present minimal differences in terms of stress. After 8 ‰ strain, though, the total damage seems to affect the behavior. Specimen with higher combined damage index (d_v) present descending branch (D_mR_c-3). The dissipated energy up to peak stress and on the whole is shown in Fig. 12. It is remarkable that in highly damaged sections (D_mR_c-2), the dissipated energy is lower both up to the peak stress and up to the total strain (25% and 30% respectively) comparing to the non-repaired specimen (R_c-2).

The repaired construction damages seem to affect similarly specimens designed with ductility requirements (Fig. 13). The maximum stress is obtained at 5 up to 6 ‰ strain. It is evident in higher levels of damage (D_mR_c-5) the peak stress is more reduced (22 %). It should be noted that when the impairment of the section exceeds 25 % (D_mR_c-5) the failure happens after 5 ‰ axial strain with abrupt reduction due to early buckling of the longitudinal reinforcement (Fig. 11). The dissipation of energy, again, both up to peak and totally of the repeated loading, is lower than the non-damaged one. Speaking of the same levels of section impairment, specimens with stirrups of minimum levels of modern design (D_mR_c-1, D_mR_c-4) dissipate slightly higher ratio of energy up to peak load than the ones with older codes (D_mR_c-1, D_mR_c-3), but 25 % and 8 % respectively higher energy on the whole. In both classifications (ω_{wc}=0.075, ω_{wc}=0.15) all specimens, damaged or not, exceed the 50 % of their capacity in dissipating energy up to the peak point of the stress-strain curve (Fig. 12).

The tendency of highly damaged specimens (d_s index) to present resistance in lower stress than designed is illustrated graphically (Fig. 13) in order to examine the dispersion in both classifications. It's sure enough that the declination is in tolerable limits, the dispersion factor (R_2) for both levels of ductility, low and high, is quite satisfactory (0.68 & 0.63 respectively).

4 PERFOMANCE OF RETROFITTED SPECIMENS

Specimens of the second category, to wit, designed according to new codes' regulations for mechanical ratio of confinement (ω_{wc}=0.15), were selected for retrofitting with RC jackets. Specimens with repaired initial construction damages are compared with identical ones without damages in terms of the different reinforcement crossing the interface between old and new concrete (Fig. 15). The initial elastic branch of the (construction) damaged specimen (B-$D_mR_cR_j$-3) almost coincides with the one containing dowels (B-$R_cR_jD_b$-7). Though, after 5 ‰ axial strain (2.5 mm-0.098 in) where the maximum resistance load is achieved, the undamaged presents 18 % higher load up to 40 ‰ axial strain (20 mm). Thereupon, the descending branches again almost coincide.

4.1 Interface reinforcement effect

In addition to, there is strong difference between these specimens and the one with welded longitudinal bars of core and jacket (Fig. 18). The last one presents almost 3 times higher initial stiffness. The maximum capacity load is achieved in 53% lower axial strain (3.2 ‰ or 1.6 mm- 0.063 in) and then up to 25 ‰ axial strain (12.5 mm- 0.492 in) the load remains 18 % lower than the one with dowels. Still, it is 6 % higher in all deformations than the damaged column. After 30 ‰ (15 mm- 0.555 in), the welded jacketed column presents up to 25 % higher load than the one with dowels or the damaged one. The repaired columns without reinforcement on the interface and small percentages of repaired section seem to have small influence in the final behavior (*B*-$D_mR_cR_j$-3) (Fig. 12).

On the other hand, on higher percentages of repaired section and on the presence of dowels (Fig. 14, *B*-$D_mR_cR_jD_b$-4), the behavior seems to be slightly different. The maximum resistance load (5 % lower) is found in almost twice the axial strain of a healthy column (*B*-$R_cR_jD_b$-8). However, the rate of reduction (r_p), of peak load in every next strain ($dP_{peak}/d\varepsilon$) is blunter in the damaged specimen (Fig. 16, Fig. 17). The secant stiffness of the damaged specimen is lower.

4.2 Load pattern effect

In Load Pattern *D* (Fig. 18), simulating the monolithic behavior of the retrofitted element, the first branch of the damaged column coincides with the undamaged one (*D*-$R_cR_jD_b$-6) up to 7 ‰ axial strain (3.5 mm). Now, the damaged column (*D*-$D_mR_cR_jD_b$-5) contains dowels crossing the interface and presents 17 % lower maximum load achieved in the same values of axial strain (7.5 ‰-3.5 mm-0.138 in). Then, the resistance load is lower from 13 % up to 19 %. Specimen with welded bars crossing the interface (*D*-$R_cR_jD_w$-7) presents 30 % higher initial stiffness comparing to the other two specimens.

The maximum resistance load is at the same levels with the undamaged column containing dowels and happens in the same values of axial strain (10.5 ‰-5.27 mm). Though, from these values of axial strain and on, the undamaged column presents a less steep descending branch. In fact, after 10 ‰ (5 mm), the welds seem to lose their capacity comparing to dowels and the load remains 17 % lower.

This Load Pattern enables higher values of maximum load and load throughout the whole spectra of axial strain due to the fact that the jacketed area is loaded directly and its capacity starts to act immediately. On the other hand, in Load Pattern *B*, the values of load are smaller since the jackets' mechanisms (confinement) are not activated until the load is entirely distributed to the jacket. In fact, in Load Pattern *B* it is proven that load is fully distributed to the jacketed area. As a result, the shear mechanisms of the interface are fully activated.

4.3 Failure modes

In both Load Patterns *B* and *D*, due to the bars crossing the interface that are welded to the longitudinal ones, there are no plastic regions throughout the loading procedure. It is remarkable though, that the load is reduced in smaller values of deformation comparing to the one containing dowels. The reduction of about 270 kN takes place in Load Pattern *B* owing to the buckling of the longitudinal bars of both core and jacket that lead to the descending branch (Fig. 19). In contrary, the presence of dowels creates damaged areas around the bar (plastic regions) decreasing the capacity of the element to carry loads (Fig. 20).

In Load Pattern *D*, the reduction is higher due to the plastic regions around the steel bar created throughout loading. The direct loading of both core and jacket lead to the activations of all kind of strength mechanisms (confinement of both core and jacket, shear mechanisms along the interface) and to higher values of load. In both Load Patterns, after 20 mm (40 ‰) displacement dowels and welds result to the same values of resistance load. Hence, thereupon, all mechanisms capacities are depleted and specimens present a remaining resistance. Table 2 resumes all measured results.

5 CONCLUSIONS

Based on the results of this experimental investigation, the following conclusions are drawn:

1. The resistance of the strengthened specimens was significantly higher than the original ones.

2. Initial damages affect the final behavior of the retrofitted specimen achieving lower values of load.

3. The presence of dowels increases the maximum load on a damaged column and lead to a stepper descending branch.

4. Specimens containing dowels presented plastic regions around the connector bars which is the mechanism of failure of the interface in high levels of displacement.

5. Welded bars increase the initial stiffness of the upgraded element but due to the buckling the secant stiffness is reduced without loss on the peak load.

It is desirable to test specimens with special treatment of the interface to investigate the chipping effect to the shear resistance of a jacketed element. This kind of research would benefit the understanding of the shear mechanisms along interfaces surfaces along with a numerical simulation. The further and more accurate quantification of damage is intended to be applied with computational methods and more experimental research.

ACKNOWLEDGMENT

The authors wish to thank Sika Hellas for providing the resins.

REFERENCES

[1] Priestley M.J.N., Seible F., Calnvi G.M., "Seismic Design and Retrofit of Bridges'', John Wiley&Sons Inc., 1996.

[2] Fardis M.N., "Seismic Design, assessment and retrofitting of concrete buildings, based on EN-Eurocode 8'', Geotechnical, geological and earthquake engineering, Springer, 2009.

[3] Bousias S., Spathis A.L., Fardis N.M. (August 1 – 6/2004), "Seismic retrofitting of columns with lap - slices via RC jackets", 13th World Conference on Earthquake Engineering, Vancouver, Canada, Paper No 1937.

[4] Vandoros G.K., Dritsos E.S. (2006(a)), "Concrete jacket construction detail effectiveness when strengthening RC columns", Elsevier – Science Direct, Construction and Building Materials 22, 264 – 276.

[5] Ersoy U., Tankut A.T., Suleiman R., "Behavior of jacketed columns", ACI Structural Journal, Vol. 90-S30, No. 3, May – June 1993.

[6] Júlio, E. S.; Branco, F.; and Silva, V. D., "Structural Rehabilitation of Columns Using Reinforced Concrete Jacketing," Progress in Structural Engineering and Materials, V. 5, No. 1, John Wiley & Sons Ltd., 2003,pp. 29-37.

[7] Rodriguez, M., and Park, R., "Seismic Load Tests on Reinforced Concrete Columns Strengthened by Jacketing," ACI Structural Journal, V. 91, No. 2, Mar.-Apr. 1994, pp. 150-159.

[8] Tasios P. Theodossius, Vitzileou Elisabeth. (1987), "Cocrete-to-Concrete Friction." Journal of Structural Eng.

[9] Bett, B. J.; Klingner, R. E.; and Jirsa, J. O., "Lateral Load Response of Strengthened and Repaired Reinforced Concrete Columns" ACI Structural Journal, V. 85, No. 5, Sept.-Oct. 1988, pp. 499-508.

[10] Júlio, E. S.; Branco, F.; and Silva, V. D., "Concrete-to-Concrete Bond Strength: Influence of the Roughness of the Substrate Surface", Construction and Building Materials, V. 18, No. 9, 2004, pp. 675-681.

[11] Júlio, E. S.; Branco, F.; and Silva, V. D., "Concrete-to-Concrete Bond Strength: Influence of an Epoxy-Based Bonding Agent on a Roughened Substrate Surface" Magazine of Concrete Research, V. 57,No. 8, 2005, pp. 463-468.

[12] Choi Dong-Uk, James O. Jirsa, David W. Fowler, "Shear Transfer across Interface between New and Existing Concretes Using Large Powder-Driven Nails", ACI Structural Journal March-April 1999

[13] Vitzileou E.N., Tasios T.P. (1987), "Behaviour of Dowels under Cyclic Deformations" ACI Structural Journal

[14] Júlio, E. S.; Branco, F.; and Silva, V. D., "RC Jacketing—Interface Influence on Monotonic Loading Response" ACI Structural Journal, V. 102,No. 2, Mar.-Apr. 2005, pp. 252-257.

[15] Júlio, E. S.; Branco, F., "RC Jacketing—Interface Influence on Cyclic Loading Response" ACI Structural Journal, V. 105,No. 4, July-August 2008, pp. 471-477.

[16] European Standard EN (2005), "Eurocode 8 Design of structures for earthquake resistance, Part 3: Assessment and retrofitting of Buildings"

[17] Organisation of Seismic Design and Protection (2012), "Greek Retrofit Code Attuned to EN 1998/3" (In Greek)

[18] American Concrete Institute (2008), "Building Code Requirements for Structural Concrete (ACI 318-08) and Commentary", ACI -318R-08 Building Code

[19] Vandoros G.K., Dritsos E.S. (2006(8), 2006(b)), "Axial preloading effects when reinforced concrete columns are strengthened by concrete jackets", Prog. Structural Engng. Mater, 79 – 92

[20] Achillopoulou D.V.; Rousakis T.C.; Karabinis I. A. (2012) , "Force transfer between existing concrete columns with reinforced concrete jackets subjected to pseudoseismic axial loading" Proceeding of 15th WCEE, Lisbon.

[21] Achillopoulou D.V.; Karabinis I. A. (2013), 'Investigation of shear transfer mechanisms in repaired damaged concrete columns strengthened with RC jackets', Structural Engineering and Mechanics, Vol. 47, No. 4, 575-598.

[22] EN 206-1: European Standard: Concrete- Part1: Specification, performance, production and conformity (December 2000), European Committee for Standardization.

[23] ACI 309R-06: Guide for Consolidation of Concrete, ACI Committee 309 (May 2006), American Concrete Institute.

[24] EN 1504: European Standard: Products and systems for the protection and repair of concrete structures - Definitions, requirements, quality control and evaluation of conformity, European Committee for Standardization, (April 2013).

Reviewers:

Doc. Ing. Pustka David, Ph.D., Department of Building Structures, Faculty of Civil Engineering, VŠB-Technical University of Ostrava. Czech Republic.

Doc. Ing. Miloš Zich, Ph.D., Institute of Concrete and Masonry Structures, Faculty of Civil Engineering, Brno University of Technology. Czech Republic.

TABLES AND FIGURES

List of tables:

Tab. 1: Specimens' characteristics
Tab. 2: Damage indexes of specimens (cores)
Tab. 3: Experimental Results of Retrofitted Specimens

List of Figures:

Fig. 1: Cores' reinforcement details
Fig. 2: Construction Damages D_mR_c-5
Fig. 3: Experimental Setup
Fig. 4: Reinforcement details of jacketed specimens
Fig. 5: Load Patterns' Shape
Fig. 6: Confinement Effect
Fig. 7: Damage indexes definition
Fig. 8: Construction damage effect on repaired columns with low ductility requirements
Fig. 9: Dissipated energy of low ductility columns: peak stress-totally
Fig. 10: Construction damage effect on repaired columns designed with ductility requirements
Fig. 11: Buckling of longitudinal bar of D_mR_c-5_ω_c=0.15 after loading.
Fig. 12: Dissipated energy of columns with ductility requirements: peak stress-totally.
Fig. 13: Association of maximum normalized resistance load (v) with the level of the (construction) damaged section ds (%)
Fig. 14: Axial Load (kN) vs Deformation δ (mm) chart for Load Pattern *B*
Fig. 15: Axial Load (kN) vs Deformation δ (mm) chart for Load Pattern *B*
Fig. 16: Rate of reduction of maximum load in plastic strain_ Load Pattern *B*
Fig. 17: Definition of r_p rate of reduction
Fig. 18: Axial Load (kN) vs Deformation δ (mm) chart for Load Pattern *D*
Fig. 19: Buckling of the longitudinal bar_ welds 4Ø8
Fig. 20: Plastic region around the dowel bar- cut of specimen

Tab. 1: Specimens's characteristics

				Connectors		
Specimens	Construction damages	ω_{wc}	ω_{wj}	Dowels	Welded bend down	Load Pattern

					bars	
B-$D_mR_cR_j$-3	√	0.15	0.035	-	-	*B*
B-$R_cR_jD_b$-7	-	0.15	0.035	6Φ10	-	*B*
B-$R_cR_jD_w$-9	-	0.15	0.035	-	4Φ8	*B*
B-$D_mR_cR_jD_b$-4	√	0.15	0.142	6Φ10	-	*B*
B-$R_cR_jD_b$-8	-	0.15	0.142	6Φ10	-	*B*
D-$D_mR_cR_jD_b$-5	√	0.15	0.035	6Φ10	-	*D*
D-$R_cR_jD_b$-6	-	0.15	0.035	6Φ10	-	*D*
D-$R_cR_jD_w$-7	-	0.15	0.035	-	4Φ8	*D*
Note:						
B/*D*: Load Pattern Shape		D_m: Construction Damages			D_b: Dowel bar	
R_c: Reinforced core		R_j: Reinforced jacket			D_w: Welded bar	

Tab. 2: Damage indexes of specimens (cores)

Specimen	ω_{wc}	ω_{wj}	d_s (%)	d_v (%)
R_c-2	0.075	-	-	-
D_mR_c-1	0.075	25	10	32
D_mR_c-2	0.075	31	14	40
D_mR_c-3	0.075	25	14	35
D_mR_c-4	0.075	13	14	25
R_c-1	0.15	-	-	-
D_mR_c-1	0.15	25	20	40
D_mR_c-3	0.15	13	24	34
D_mR_c-4	0.15	25	28	46
D_mR_c-5	0.15	37	26	54
D_mR_c-6	0.15	31	22	46
ω_{wc}= mechanical percentage of stirrups				

Tab. 3: Experimental Results of Retrofitted Specimens

	Cores				Jackets			
Specimens	δ_{peak}	δ_u	P_{peak}	E_{ntot}	δ_{peak}	δ_u	P_{peak}	E_{ntot}

	(mm)	(mm)	(kN)	(MJ/m^3)	(mm)	(mm)	(kN)	(MJ/m^3)
B-$D_mR_cR_j$-3	3.25	4.92	525.49	0.13	3.78	52.23	814.22	1.79
B-$R_cR_jD_b$-7	3.50	3.50	533.00	0.13	2.50	44.60	876.38	1.90
B-$R_cR_jD_w$-9	4.65	4.25	599.18	0.10	1.58	87.98	1127.72	2.96
B-$D_mR_cR_jD_b$-4	3.90	5.45	441.90	0.18	6.20	50.95	1062.98	2.90
B-$R_cR_jD_b$-8	3.60	4.85	612.00	0.12	3.17	145.94	1110.78	6.83
D-$D_mR_cR_jD_b$-5	7.00	10.00	553.29	0.15	3.75	36.00	2111.24	0.70
D-$R_cR_jD_b$-6	-	.	-	-	4.73	43.38	922.34	1.62
D-$R_cR_jD_w$-7	-	.	-	-	5.87	46.54	876.39	1.75
Note:	δ_{peak}: deformation corresponding to peak load							
	δ_u: deformation corresponding to 20% of the peak load							
	P_{peak}: peak load (maximum presented load)							
	E_{ntot}: total absorbed energy							

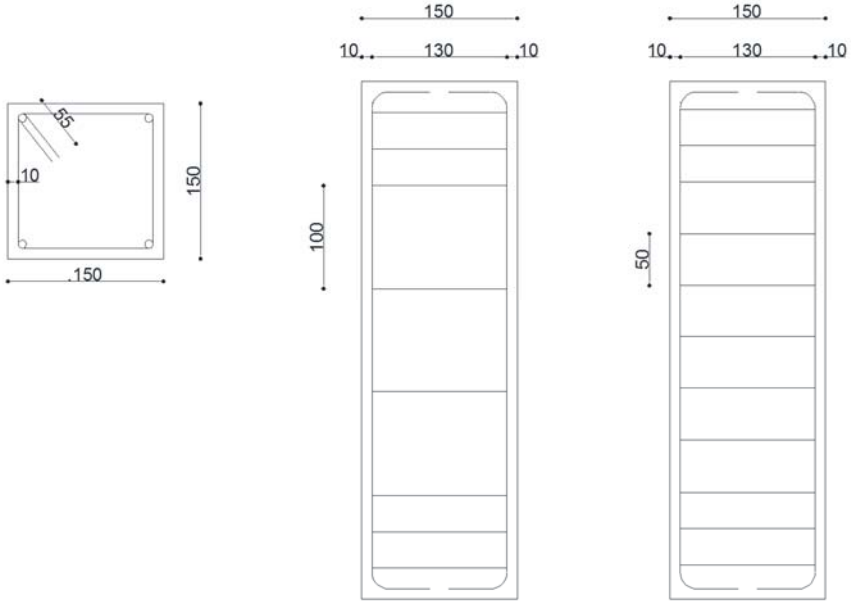

Fig. 1: Cores' reinforcement details (mm)

Fig. 2: Construction Damages_D_mR_c-5

Fig. 3: Experimental Setup

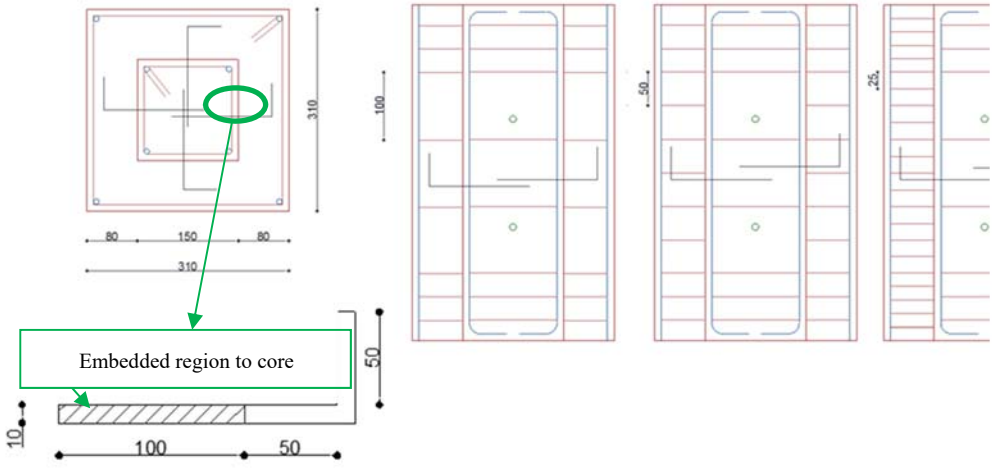

Fig. 4a: Jacketed specimens containing dowels (mm)

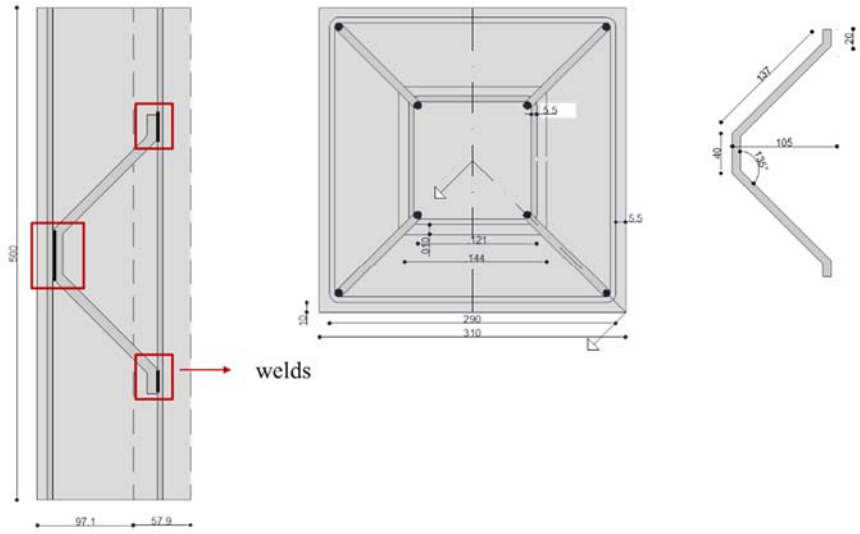

Fig. 4b: Jacketed specimens containing welded-bend down bars (mm)

Fig. 4: Reinforcement details of jacketed specimens

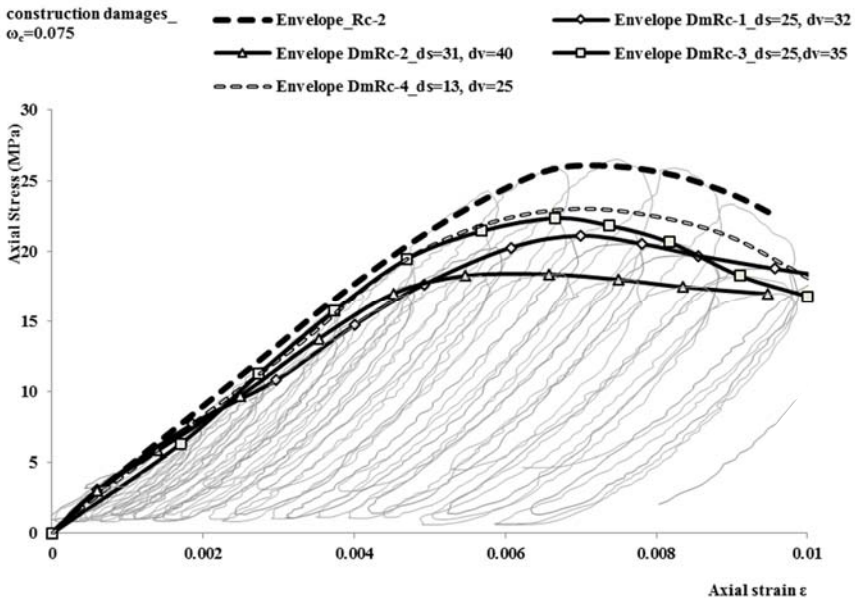

Fig. 5: Construction damage effect on repaired columns with low ductility requirements

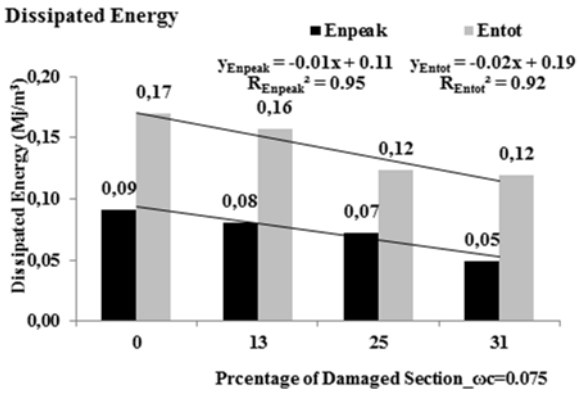

Fig. 6: Dissipated energy of low ductility columns: peak stress-totally

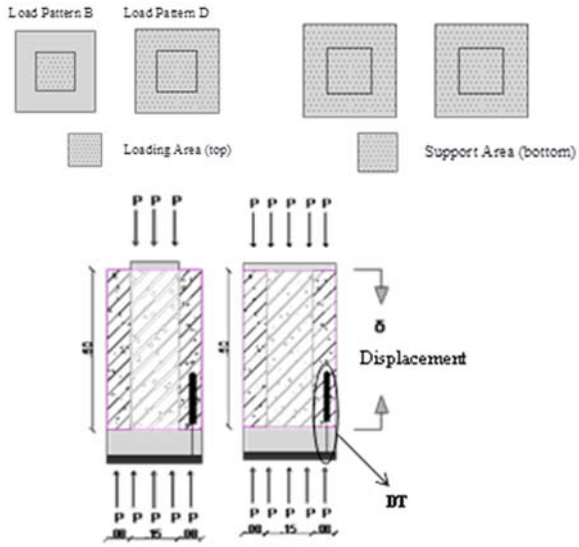

Fig. 7: Load Patterns' Shape

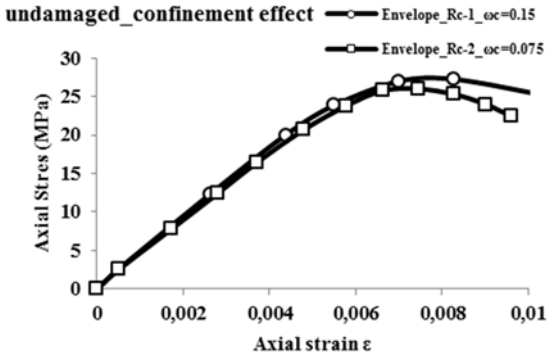

Fig. 8: Confinement Effect

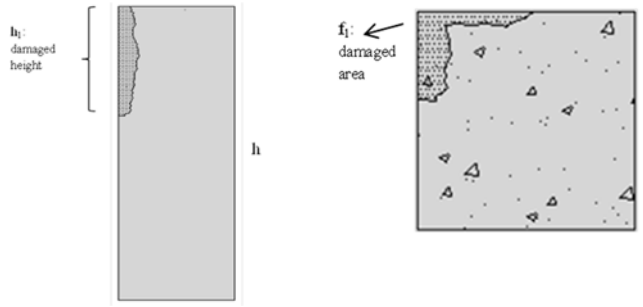

Fig. 9: Damage Indexes definition

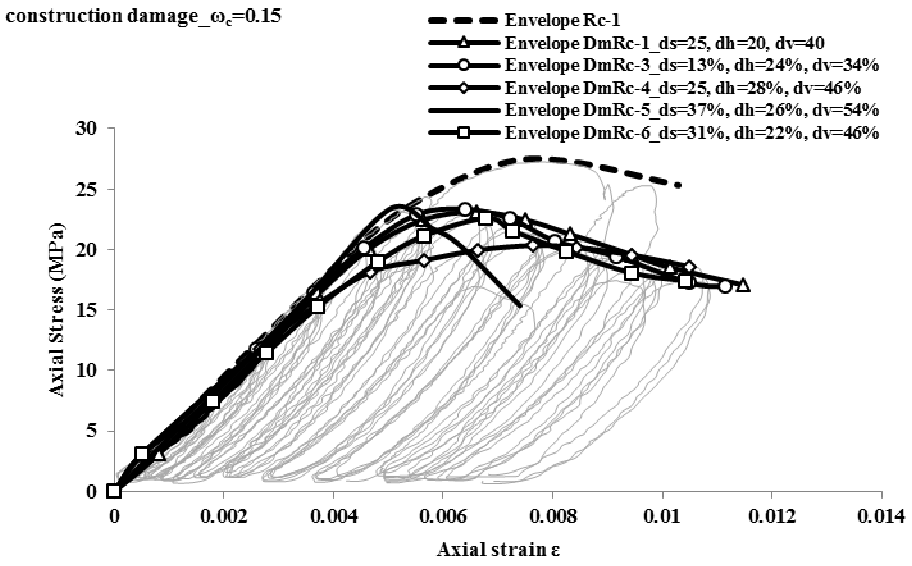

Fig. 10: Construction damage effect on repaired columns designed with ductility requirements

Fig. 11: Buckling of longitudinal bar of D_mR_c-5_ω_c=0.15 after loading

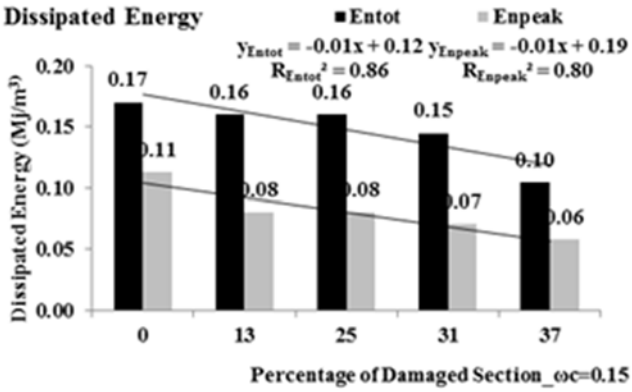

Fig. 12: Dissipated energy of columns with ductility requirements: peak stress-totally

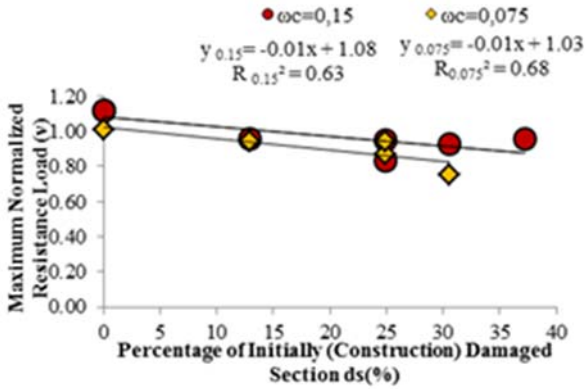

Fig. 13: Association of maximum normalized resistance load (v) with the level of the (construction) damaged section d_s (%)

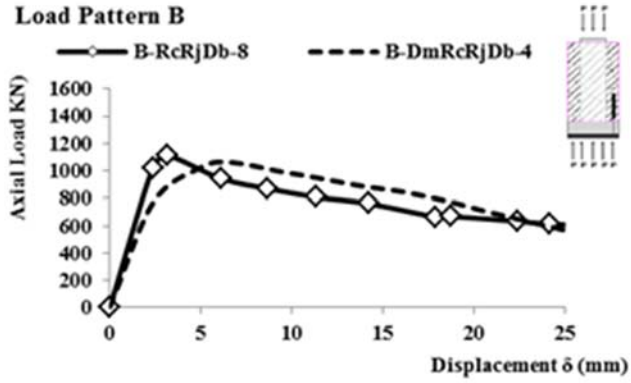

Fig. 14: Axial Load (kN) vs Deformation δ (mm) chart for Load Pattern B

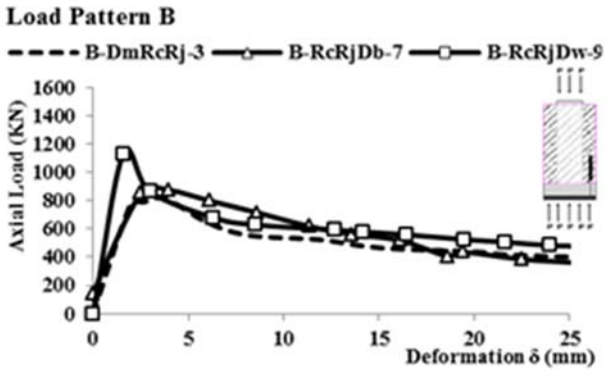

Fig. 15: Axial Load (kN) vs Deformation δ (mm) chart for Load Pattern *B*

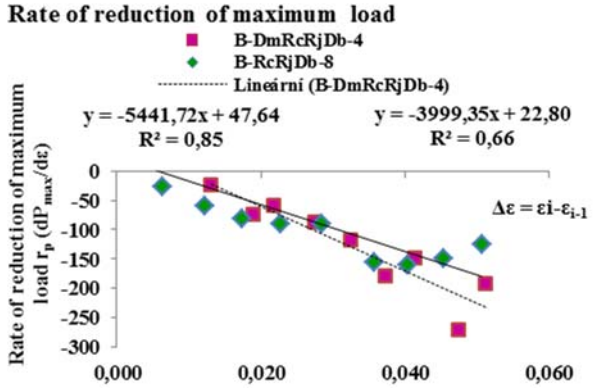

Fig. 16: Rate of reduction of maximum load in plastic strain - Load Pattern *B*

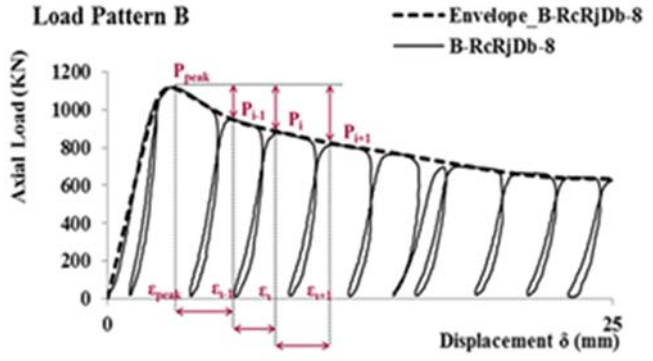

Fig. 17: Definition of r_p rate of reduction

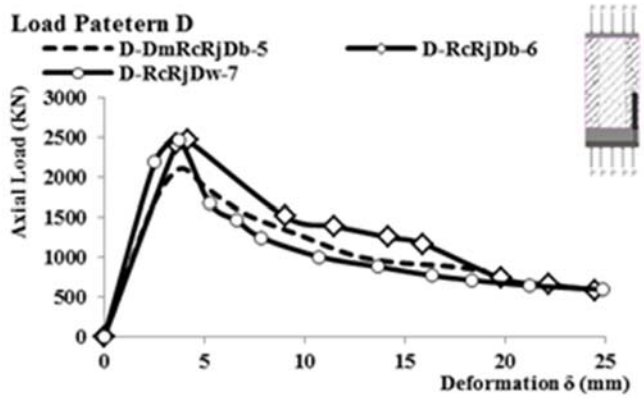

Fig. 18: Axial Load (kN) vs Deformation δ (mm) chart for Load Pattern *D*

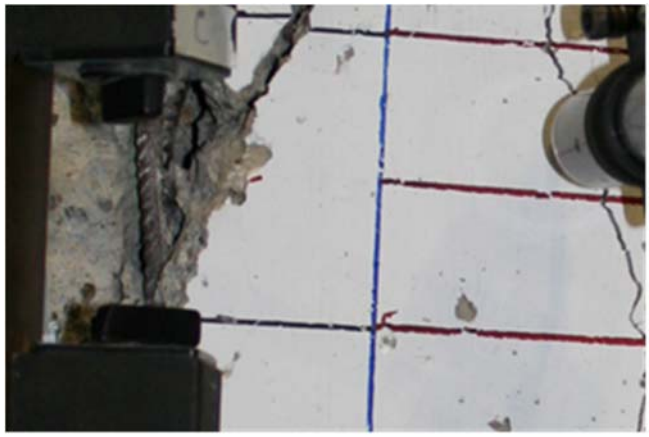

Fig. 19: Buckling of the longitudinal bar welds 4Ø8

Fig. 20: Plastic region around the dowel bar - cut of specimen